Vertically migrating *Isoxys* and the early Cambrian biological pump

Stephen Pates[1,2]*, Allison C. Daley[3], David A. Legg[4], and Imran A. Rahman[5]

[1]Museum of Comparative Zoology and Department of Organismic and Evolutionary Biology, Harvard University, USA

[2]Department of Zoology, University of Cambridge, UK

[3]ISTE, University of Lausanne, Switzerland

[4]Faculty of Science and Engineering, University of Manchester, UK

[5]Oxford University Museum of Natural History, University of Oxford, UK

*sp587@cam.ac.uk

Abstract

The biological pump is crucial for transporting nutrients fixed by surface-dwelling primary producers to demersal animal communities. Indeed, the establishment of an efficient biological pump was likely a key factor enabling the diversification of animals over 500 million years ago during the Cambrian explosion. The modern biological pump operates through two main vectors: the passive sinking of aggregates of organic matter, and the active vertical migration of animals. The coevolution of eukaryotes and sinking aggregates is well understood for the Proterozoic and Cambrian, however little attention has been paid to the establishment of the vertical migration of animals. Here we investigate the morphological variation and hydrodynamic performance of the Cambrian euarthropod *Isoxys*. We combine elliptical Fourier analysis of carapace shape with computational fluid dynamics simulations to demonstrate that *Isoxys* species likely occupied a variety of niches in Cambrian oceans, including vertical migrants, providing the first quantitative evidence that some Cambrian animals were adapted for vertical movement in the water column. Vertical migration was one of several early Cambrian metazoan innovations that led to the biological pump taking on a modern-style architecture over 500 million years ago.

Key words: biological pump; Cambrian; computational fluid dynamics; *Isoxys*; pelagic

Introduction

The biological pump is the process by which organic nutrients are transported from shallow ocean to deep sea [1]. Today this consists of two major vectors: passive sinking of organic matter aggregates and vertical movement of animals [1] (**Fig 1**). The biological pump, the main driver of the marine carbon cycle, is responsible for approximately two thirds of the vertical gradient of carbon in the ocean [2]. While transport of carbon to the deep ocean through vertical mixing of dissolved organic carbon (DOC) carries significant amounts of carbon to depth, 95% of DOC cannot be used as food by marine organisms [1,3]. In contrast, aggregates and vertical migrants concentrate organic matter in a form that can be utilized by demersal animals [1] and are therefore crucial for the establishment and sustenance of deep-water communities.

The biological pump was very different before the Cryogenian Period (>720 Ma). Cyanobacterial picoplankton (0.2–2.0 µm) domination led to a stratified and turbid water column [e.g. 4–6]. Cells were too small to sink in significant numbers, so most nutrients were recycled within the surface waters, with little export to the deeper ocean [4–6]. The flux of the aggregation vector (**Fig. 1**) would have increased when primary productivity shifted to be eukaryote-dominated during the Cryogenian ~650 Ma [7], and further when Cambrian suspension feeding sponges and pelagic phytoplanktivores applied a size-selective pressure for larger primary producers [8–12]. The carcasses, sloppy feeding, and faecal pellets of macrozooplankton, including phytoplanktivorous crown-group crustaceans [e.g. 9], would have further increased the formation and size of aggregates, and thus the flux along this vector. However, despite the importance of vertical migration in the transport of nutrients necessary to sustain mesopelagic and deep-water ecosystems in the modern ocean [e.g. 13], this vector is poorly understood in the Cambrian.

Comparisons of the morphology of Cambrian fossil organisms with modern vertically mobile pelagic animals provides the opportunity to infer whether vertical migration occurred in oceans over 500 million years ago. Qualitative comparisons between the pelagic crustacean *Gnathophausia* and the nektonic stem group euarthropod [14] *Isoxys* [e.g. 15,16] suggest the latter is a promising candidate. The 20 *Isoxys* species so far formally described are united by the presence of a bivalved carapace which bears both anterior and posterior spines [17] (**Fig. 2**), and the genus has a cosmopolitan distribution [e.g. 18]. The presence of eyes that comprise ~10% of the body length, a digestive tract with paired serial midgut glands, and a pair of anteriorly positioned raptorial appendages (**Fig. 2)** support a predatory habit for *Isoxys*, which would have been well-suited for capturing small soft-bodied invertebrates [19]. *Isoxys* is unusual for Cambrian animals as a pelagic lifestyle has been proposed [e.g. 18], although some recent workers have suggested a potential

hyperbenthic lifestyle (1–10 m above the bottom), with individuals capable of moving small distances vertically [19,20]. However, while *Isoxys* carapaces appear to show adaptations for hydrodynamic streamlining, interspecific differences in both carapace asymmetry and spine lengths (e.g. **Fig. 2**), as well as soft parts, suggest that different species may have occupied distinct niches, including some much closer to the seafloor [21].

Here, we provide the first quantitative assessment of carapace shape variation across the group and compare *Isoxys* to other Cambrian 'bivalved' euarthropods and *Gnathophausia*. Subsequently, through computational fluid dynamics simulations, we test the importance of the spines and carapace outline for generating lift and reducing drag, and thus the ability of different taxa to move vertically through the water column. These analyses support the hypothesis that *Isoxys* taxa occupied a variety of distinct niches in Cambrian oceans, including vertical migrants.

Materials and methods

Outline analyses

Two-dimensional outlines of 20 *Isoxys* species, its sister taxon *Surusicaris elegans* [22], 6 *Tuzoia* species, and 11 *Gnathophausia* species were constructed in Inkscape from literature sources by SP (Supplementary Table 1) and imported into R [23] for elliptical Fourier analysis (EFA). DAL independently constructed 20 *Isoxys* and 1 *Surusicaris* outlines directly from photographs of fossil specimens to allow assessment of the error introduced in the creation of outlines (Supplementary Table 2; Supplementary Materials 1). *Tuzoia* was chosen for comparison as it is also common in Cambrian communities, and has been suggested to be closely related to *Isoxys* based on similarities in the structure of the eyes and carapace shape [e.g. 24]. *Gnathophausia* was selected because similarities in the carapace morphology of one species (*G. zoea*) and *Isoxys* have been repeatedly noted [e.g. 16,19], the carapaces of these animals are similar in size (10–30 mm), and multiple species of *Gnathophausia* are known to be vertically mobile in the modern ocean, having been sampled from surface waters and at depths of over 3000 meters [25].

Outlines were sampled at the same resolution (64 points provided sufficient detail to distinguish taxa), centred, scaled by centroid size, and subjected to EFA using the *Momocs* package [26]. Harmonics describing 99.9% of the variation were retained. EFA results were visualized with a Principal Components Analysis. A hierarchical clustering analysis (cluster package; [23]) quantitatively grouped similarly shaped carapaces together using all principal components.

Computational fluid dynamics

Isoxys species reflecting the variation in carapace shape over both PC1 and PC2 were chosen for inclusion in computational fluid dynamics simulations, and *Gnathophausia zoea* was analysed for comparison. We chose to undertake a two-dimensional analysis to conserve computational resources and minimize errors in the modelled geometries (the exact three-dimensional shape is unknown for most taxa). This is justified because undeformed *Isoxys* specimens preserved in dorsal view show a narrow profile [16,21,27,28]. Propulsion during swimming derived from movement of the ventral appendages, and not from flapping of the bivalve carapace [15, 27]. A lack of adductor muscles means that *Isoxys* was unable to alter the size of the gape during swimming [15], and the numerous specimens preserved in 'butterfly' orientation are considered exuviae [27]. In addition, the full variation of the carapaces considered in this study can be visualized in two dimensions. Two-dimensional analyses are commonly performed on analyses of wing outlines to assess aerodynamic performance by both biologists and engineers, [e.g. 29,30]. A 2D analysis is suitable for this study as

105 the wake behind the *Isoxys* carapaces is steady at the Reynolds numbers considered, so can be
106 modelled with two-dimensional simulations [32, 34]. The impact of soft parts such as eyes
107 protruding from the carapace was analysed for two taxa: *Isoxys acutangulus* and *I. longissimus.*
108 *Isoxys* was assumed to be negatively buoyant, like *Gnathophausia* [31]. All *Isoxys* species were
109 assumed to have the same carapace composition and density. The cuticle ornamentation in some
110 *Isoxys* species is not expected to impact the drag at the low Reynolds numbers considered in this
111 study, as the roughened surface falls within the slowly moving fluid near the carapace surface [32].

112 Following validation and verification of the model and setup for low Reynolds numbers, and
113 mesh quality assessments using ANSYS Mesh and ANSYS Fluent (*Ansys® Academic, Release 2020 R2*;
114 Supplementary Materials 2), outlines of the selected *Isoxys* species and *G. zoea* were exported from
115 R as .txt files readable by ANSYS DesignModeler (*Ansys® Academic, Release 2020 R2*; Supplementary
116 Materials 2), and standardized to a dorsal length (chord length) of 25 mm. This allowed size-
117 independent comparisons of hydrodynamic performance of shapes. While some *Isoxys* taxa (e.g. *I.*
118 *communis*, *I. longissimus*) can reach up to 50 mm, other adult forms only reach ~20 mm (e.g. *I.*
119 *glaessneri*, *I. volucris*) [18,27]. A size of 25 mm represents a compromise size for comparison
120 between these larger and smaller forms, with the influence of larger size able to be assessed by
121 simulating higher Re (as Re depends on both size and swimming speed).

122 Computational fluid dynamics (CFD) simulations were conducted using the steady-state
123 laminar solver in ANSYS Fluent (*Ansys® Academic, Release 2020 R2*). The laminar solver performed
124 best of the three considered during validation and verification (laminar, SST, k-epsilon;
125 Supplementary Materials 2), as expected for the low Reynolds numbers in this study [32].

126 Coefficients of drag (Cd) and lift (Cl) (Supplementary Materials 2) were calculated under
127 three flow speeds equating to 0.75, 1.00 and 1.18 body lengths per second (chord Reynolds
128 numbers, Re, 255, 340, and 400 respectively for saltwater conditions at 0˚C; Supplementary
129 Materials 2). These Re were chosen as swimming speeds of between 75% and 100% of the body
130 length per second have been observed in adult *Gnathophausia ingens* (carapace mean length ~25
131 mm; [33]), and as the laminar model was validated against published drag and lift data for NACA
132 airfoils at exactly Re = 400 [29]. The chord length (25 mm) was taken as the reference area for both
133 coefficients.

134 Solutions were considered converged when residuals were $<10^{-6}$. Simulations were run at
135 numerous angles of attack, to evaluate the hydrodynamic performance of carapaces at multiple
136 orientations. In tank experiments, *Gnathophausia ingens* has been observed to change angle of
137 attack to generate more lift or less drag at different swimming speeds [33]. The angle of attack was

138 increased from 0–8˚ at all Re, until the stall angle could be identified and/or unsteady flow was
139 observed. If the stall angle was not reached, further experiments were run until the maximum lift
140 coefficient was obtained. Negative angles of attack were also simulated to assess the negative lift
141 generated by the different outlines. In all cases, the absolute value of the negative angle of attack
142 was increased until the drag coefficient was equal to or greater than that of the stall angle. When
143 unsteady flow was suspected to be the reason that steady state simulations did not converge, the
144 steadiness of the flow field was determined by carrying out a time-dependent analysis of 100 time
145 steps, with each time step equal to the flow speed (so, for an inlet velocity of 0.01875 ms^{-1}, the time
146 step = 0.01875 s).

147

Results

Outline analysis

In the outline analysis, a total of 18 harmonics were retained. Principal coordinates 1 and 2 described 79.3% of the total variation. Carapace asymmetry, narrowness, and spine length increased as PC1 became more positive, while the length of the anterior spine relative to the posterior spine corresponded to an increase in PC2 (**Fig. 3**). *Isoxys* occupied the largest area in the morphospace. Visual overlap of the areas occupied by the genera demonstrated that some *Isoxys* taxa were more similar in shape to *Gnathophausia* than their Cambrian relatives *Surusicaris* and *Tuzoia*. Confirmation was provided by the cluster analysis (**Fig. 3**). All six *Tuzoia* species formed a single cluster, with *Isoxys* taxa spread over the three remaining groups (*Surusicaris* group, *Gnathophausia* groups 1 and 2). Species clustered with *Surusicaris* have symmetric and deep carapaces and relatively short spines. Species in the *Gnathophausia* groups displayed narrower outlines whose narrowness, asymmetry and spine length increased with PC1. The single species of *Isoxys* in *Gnathophausia* group 1, *I. paradoxus*, displayed an anterior spine much more elongate than its posterior one, that contrasted with the seven species in *Gnathophausia* group 2 with their spines of approximately equal length.

Computational fluid dynamics

Computational fluid dynamics simulations assessed the impact of increasing asymmetry, spine length, and relative lengths of anterior and posterior spines on hydrodynamic performance. Inclusion of eyes did not significantly impact the hydrodynamic performance of carapaces (Supplementary Materials 3). *Isoxys zhurensis*, the most symmetric species chosen for analysis, created an unsteady wake with Kármán vortex street at the lowest Re considered, and so no drag or lift coefficients were obtained (Supplementary video). The flow around remaining *Isoxys* outlines was laminar with a steady wake, and there was no evidence for three dimensionality (Supplementary Materials 4). Greater asymmetry and narrowness (more positive in PC1, **Fig. 3**) resulted in lower drag coefficients, as demonstrated by a comparison of the short-spined taxa *I. chilhoweanus*, *I. acutangulus*, and *I. mackenziensis.* The most asymmetric of these forms, *I. mackenziensis*, produced lower drag coefficients than the other two, but ranges of lift coefficients were similar for all three (**Fig. 4a**). More elongate spines increased the range of lift coefficients (vertical bars, **Fig. 4a**) and, significantly, negative lift coefficients at negative angles of attack (e.g., compare *I. mackenziensis*, *I. communis*, and *I. longissimus*). In *I. paradoxus,* where the anterior spine is much longer than the posterior one (more positive in PC2, **Fig. 3**), the range of lift coefficients further increased (**Fig. 4a**). Similar drag coefficients and ranges of lift coefficients were obtained in

an analysis of the hydrodynamics of *Gnathophausia zoea*, when either the carapace alone or both the carapace and abdomen were considered (**Fig. 4b**).

Discussion

Vertical migrations and niche partitioning in Isoxys

Functional morphology of *Isoxys* fossil specimens supports an off-bottom (hyperbenthic or pelagic) life habit for this animal [15,16,18,19,34], based on the eye orientation (forwards, slightly ventral) and the elongate slender carapace shape of *Isoxys*. Our study combines outline morphometric and computational fluid dynamics analyses and suggests that *Isoxys* species occupied a variety of niches, including some as pelagic vertically mobile predators.

Lift and drag coefficients of *Isoxys* carapaces indicate variation in the depth range and swimming speeds of these species. *Isoxys* taxa clustering with *Surusicaris* (**Fig. 3**) generate positive lift, but do not generate negative lift (**Fig. 4**). This supports suggestions of previous workers that these *Isoxys* species may have occupied a hyperbenthic (1–10 m above the seafloor) and/or nektobenthic [21] niche, perhaps moving vertically short distances in the water column [15,19,35]. Vertical movement would be achieved by altering the angle of attack to produce lift force greater than (ascent), equal to (horizontal swimming), or less than (descent) the impact of their negative buoyancy. Drag reduction associated with streamlining would have allowed some taxa (e.g., *I. mackenziensis*) to capture faster-moving prey animals, as faster swimming speeds could have been maintained over longer distances for the same metabolic cost.

Isoxys species clustering with *Gnathophausia* show convergent adaptations to moving vertically in the water column, such as asymmetric carapaces with elongate anterior and posterior spines (**Figs. 3, 4**). This does not preclude elongate spines from also acting as anti-predatory deterrents, as suggested by [15]. These adaptations provided hydrodynamic benefits that would have allowed the *Isoxys* species to operate over a wider bathymetric range. A streamlined carapace facilitates not only faster movement, but also more efficient swimming, beneficial for migrations over a long distance. The carapace shapes of *I. longissimus* and *I. paradoxus* generate lift coefficient ranges and minimum drag coefficients comparable to the modern crustacean *Gnathophausia zoea* (**Fig. 4**), which has been recovered at depths ranging from surface waters down to ~3000 m in the modern ocean [25]. These results also suggest that an elongate abdomen in *G. zoea* reduces the drag experienced by the animal slightly but does not greatly impact on the range of lift coefficients (**Fig. 4b**), though the abdomen may also play a physical role. Animals that move vertically in the water column do not have to cover the entire distance from the surface ocean to demersal communities, and instead sometimes migrate across only a shorter vertical distance. Thus, *Isoxys* taxa with the broadest ranges of lift coefficients (*I. longissimus* and *I. paradoxus*) likely covered a wider depth range than those with smaller ranges of lift coefficients (e.g., *I. communis*).

Corroborating evidence for variation in bathymetric range for different *Isoxys* species comes from the fossil record itself. Members of different groups as resolved in the cluster analysis (convex hulls, **Fig. 3**) co-occur with different relative abundances in Cambrian deposits preserving soft-bodied fossils. In general, species with inferred vertically migrating lifestyles are much rarer than those that lived close to the seafloor. In the Chengjiang Biota, *Isoxys auritus* (*Surusicaris* group) greatly outnumbers both *I. paradoxus* and *I. curvirostratus* (*Gnathophausia* groups 1 and 2, respectively) (**Fig. 3;** [15,21,36–38]). A similar pattern of relative abundances can be observed in the two Burgess Shale taxa (**Fig. 2**): in the Walcott Quarry, *I. acutangulus* (*Surusicaris* group) comprises nearly 0.5% of the total community, vastly outnumbering the extremely rare inferred vertical migrant *I. longissimus* (*Gnathophausia* group 2; [16,39]. The relative abundances of these *Isoxys* species can be partly explained by the differences in lifestyle predicted by the carapace outline and soft anatomy. The less hydrodynamic taxa (those with higher drag coefficients and narrower ranges of lift coefficients) likely lived near the seafloor, with the more streamlined species living in the water column and occupying a broader bathymetric range. This broader bathymetric range would have included more open water settings, beyond the maximum depth of the shelf where Cambrian deposits preserving soft-bodied fossils occur – *Gnathophausia zoea* for example has been found at depths of up to 3000 metres [25]. As modern euarthropod carapaces disarticulate quickly after death [e.g. 40], the preservation potentials for pelagic euarthropods living high in the water column are lower than for those living closer to the seafloor. In addition, animals which occupy an ecological niche in the open water are less likely to find themselves over shelf environments such as those which preserve soft-bodied fossils or be trapped and transported by an obrution event responsible for the preservation of soft bodied communities in these settings. The small numbers of vertically mobile *Isoxys* individuals observed may have been at the bottom of their vertical migrations and/or been transported horizontally by currents. *Isoxys* species are not globally distributed [41]. Many species (for example those clustering with *Surusicaris*) appear suited to hyperbenthic habits, and so would be expected to have provincial distributions. The limited geographic distribution of *I. longissimus* and *I. paradoxus* is most likely due to a combination of factors. Firstly, deposits where *Isoxys* is expected to be preserved are not evenly distributed in time and space – Stage 3 deposits are mostly in South China, while Wuliuan and younger are mostly in Laurentia [42], though the absence of the Chengjiang species *I. paradoxus* from Sirius Passet is notable. Secondly, the lower preservation potential of pelagic (compared to hyperbenthic) species means that they are rare even in Tier 1 Burgess Shale-type Lagerstätten (*sensu* [42]). However, despite its rarity, the Burgess Shale species *I. longissimus* has a wider known geographic range than the co-occurring *I. acutangulus*. The former has also been reported from the Wheeler Formation, House Range, Utah, USA [43]. The

situation appears more complex in the Emu Bay Shale, where the more hydrodynamic species *I. communis* greatly outnumbers the less streamlined *I. glaessneri* [27]. However, the Emu Bay Shale is not a traditional Burgess Shale-type deposit, instead it represents a localized deep water micro basin on the inner shelf [44]. Here fluctuating oxygen levels may have periodically deoxygenated the water column, possibly killing pelagic taxa like *I. communis* in great numbers and creating a taphonomic bias that preferentially preserves pelagic taxa.

Further support for the Chengjiang taxon *Isoxys auritus* occupying a niche closer to the seafloor than *I. curvirostratus* comes from a comparison of the soft anatomy (soft parts are unknown for *I. paradoxus*) [21]. The stout endopods of *I. auritus* appear well-suited for interacting with the substrate, while exopods with broad fringing lamellae and a sophisticated vascular system in the more streamlined *I. curvirostratus* suggest it was a more powerful swimmer, providing additional support for a pelagic habit [21].

Lastly, a compendium of fossil, geochemical, and phylogenetic data show that vertically mobile *Isoxys* species would have had access to a variety of pelagic prey items and an oxygenated water column to travel in. Cambrian oceans were not stratified, instead displaying wedge-shaped oxygen minimum zones broadly comparable to modern oceans [45]. *Isoxys* prey size range (~5–20 mm; [19]) includes Cambrian phytoplanktivores, such as crustaceans with setae and filter plates from Sirius Passet and Mount Cap (15–50 mm) [4,8,9,12], as well as crown group branchiopods and copepods and total group ostracods [46], as well as bradoriids, some of which were also likely pelagic [47,48]. The presence of planktonic larvae, another possible prey item, can be inferred from tip-dated phylogenetic analyses that support the evolution of metamorphosis in euarthropods by the Cambrian [49]. Thus, a range of different data sources suggest multiple *Isoxys* taxa were vertically mobile, and that the Cambrian ocean could support such an ecology.

Metazoans and the Cambrian biological pump

The presence of the likely vertically mobile *Isoxys paradoxus* in the Chengjiang Biota makes it the oldest confidently identified euarthropod vertical migrant, and likely among the first animals to employ this life habit. For this vector to be significant by the Cambrian Stage 3, a large biomass of *Isoxys* would need to move vertically. While pelagic animals have a lower preservation potential than benthic ones (for example very few fossil copepods are known [50]), *Isoxys* species with inferred (hyper)benthic habits are extremely abundant in both the Chengjiang and Burgess Shale [15,16,21,36–38]), and their pelagic counterparts *Isoxys longissimus* and *I. paradoxus* may have been similarly numerous. The Chengjiang and coeval Qingjiang biotas also preserve the earliest evidence

for gelatinous zooplankton, which move vertically small distances in the modern ocean [51,52]. However, an active swimming *Isoxys* would have covered greater distances more rapidly. Furthermore, the presence of a through gut would have increased processing time for food, vital for transporting nutrients consumed in surface waters to the deep ocean as faecal pellets. Vertical migration was one of many important eukaryotic and metazoan innovations key to establishing a modern-style biological pump. A series of metazoan innovations which appear in the fossil record in quick succession during the early Cambrian gave the biological pump a modern-looking structure (**Fig. 5**), which was strengthened during the Phanerozoic.

The shift to primary production dominated by eukaryotes, and the innovation of active suspension feeding, would have ventilated the oceans, cleared organic matter in the water column, and increased transfer of oxygen and plankton of increasing sizes from the surface to the sediment-water interface [e.g. 6]. The first of these events occurred during the Cryogenian [7], but while benthic passive suspension feeders are known from the Ediacaran [e.g. 53], early Cambrian stem and crown-group sponges represent the oldest benthic active suspension feeders [10,11]. As active suspension feeders, sponges were able to transport large volumes of water between benthic and pelagic realms [e.g. 54], and the most abundant sponges from the Cambrian, the reef building archaeocyaths, display pore size differentiation within reef systems [55], presumed to be evidence of prey size-selectivity. This illustrates that predator–prey feedbacks were present in the Cambrian Stage 2 (**Fig. 2**), presenting a potential driver towards a larger size of plankton, increasing the sinking speed and efficiency of this part of the biological pump, and ventilating the water column.

The invasion of the pelagic realm by eumetazoan zooplankton provides the next step towards a modern-style biological pump. These zooplankton would have further cleared surface waters and contributed faecal pellets to organic aggregates sinking to the deep ocean, and also increased oxygen levels at depth [e.g. 6,54]. The small shelly fossil (SSF) record provides a source of evidence for the invasion of the pelagic realm by eumetazoans. Terreneuvian SSFs include the possible chaetognath *Protoherzina* and the molluscs *Watsonella*, *Aldanella*, and *Oelandiella*, whose widespread distributions are suggestive of a pelagic lifestyle, or at least a planktonic larval stage (**Fig. 5)** [56]. Euarthropods, likely early occupants of the plankton [35], are represented in the SSF record from the Cambrian Stage 3 by millimetre scale bradoriids among others (**Fig. 5)** [e.g. 47,57,58]. The first macroscopic nektonic suspension feeders, such as the radiodont *Tamisiocaris,* also appear at this time [59], while the first centimetre-scale phytoplanktivores are identified close to the Stage 3–4 boundary (**Fig. 5)** [12].These data suggest that there was an increase in the diversity of millimetre-scale zooplankton at or close to the base of Stage 3, very close in time to the appearance of the first vertical migrants. Most bradoriids are considered benthic, however *Anabarochilina* increased its

distribution in three phases, providing complementary evidence for a steady strengthening of the pump during the Cambrian. In Epoch 2 *Anabarochilina* was coupled with benthic assemblages, by the Wuliuan it spread to a wider spectrum of lithofacies, and by the Guzhangian two species became widely distributed [48].

Significance of vertical migration for the early Cambrian radiation of animals

The metazoan innovation of vertical migration would have impacted both demersal and pelagic communities. The strength of the impact depends on the amount of biomass undertaking vertical migration. Models based on Cambrian environmental parameters predict that vertical migration would have increased the efficiency of the carbon pump by around 7% [60], however, more significantly, vertical migrants transport organic nutrients to the deep sea more quickly than aggregates, with a different nutritional balance, and repackage decaying sinking organic matter (**Fig. 1**) [1,13,61–64]. In addition, vertical migrants are major contributors to ocean mixing and ventilation, spreading oxygen and nutrients throughout the water column [e.g. 54,65]. These effects likely played a role in contributing to the rapid rate of diversification during the Cambrian explosion, interwoven with numerous evolutionary and ecological feedbacks. For example, the higher metabolic needs and nutrient requirements of large biomineralizing animals and motile predators [66] may have been facilitated by increased quality and quantity of nutrient transport in the biological pump, and resulted in increased oxygenation of bottom waters. In turn, the increasing size and motility of predators would have provided a further ecological pressure for animals to 'escape' into the pelagic realm.

The establishment of a biological pump with a modern-style architecture by the Cambrian Stage 3 does not mean that the fluxes along the Aggregation and Vertical Migration vectors (**Fig. 1**) remained constant to the modern day. Indeed it likely strengthened through the Palaeozoic with an increase in biomass (from an increased number of taxa, individuals, and size of individuals). Fossil evidence points to additional metazoan innovations during the Palaeozoic that would have affected the fluxes along these vectors and strengthened the pump. For example, the Aggregation vector would have been strengthened following the evolution of centimetre-scale and decimetre-scale phytoplanktivores later in the Cambrian [12,67], and the major radiation of plankton and the evolution of metre-scale nektonic suspension feeders during the Great Ordovician Biodiversification Event [68–70]. The flux of nutrients along the Vertical Migration vector would have increased as pelagic and vertically migrating animals diversified and increased in size – an innovation that would also have increased the mixing of waters and ocean ventilation. For example, the evolution of large,

fast moving fish as part of the Devonian nekton revolution is expected to have been especially significant [54,71].

In summary, the innovation of vertical migration in some *Isoxys* species was one of several interwoven and coevolutionary feedbacks during the early Cambrian that increased the efficiency and altered the architecture of the biological pump, likely contributing to the rapid expansion in metazoan diversity at this time.

354 **Acknowledgements**

355 We thank the Associate Editor, two anonymous referees, and Christian Klug, who provided helpful
356 reviewer comments. We thank members of the Ortega-Hernández Lab for Invertebrate Paleobiology
357 (Harvard University) for fruitful discussions. S. Butts (Yale Peabody Museum) and M. Florence
358 (Smithsonian National Museum of Natural History) provided curatorial assistance.

359 **Funding**

360 SP was supported by an Alexander Agassiz Postdoctoral Fellowship (Harvard University) and a
361 Herchel Smith Postdoctoral Fellowship (University of Cambridge), DAL by a Dame Kathleen
362 Ollerenshaw Research Fellowship (University of Manchester), and IAR by a Museum Research
363 Fellowship (Oxford University Museum of Natural History).

364 **Supplementary materials**

365 Are available through the Open Science Framework: doi.org/10.17605/OSF.IO/2JDRS

366 **Author contributions**

367 SP conceived the study. SP and DAL collected data on *Isoxys* carapaces. SP conducted the outline
368 analyses. SP conducted the CFD analyses with input from IAR. SP drafted the article and figures. All
369 authors interpreted the data, critically revised the article, and approved the final version.

References

1. Turner JT. 2015 Zooplankton fecal pellets, marine snow, phytodetritus and the ocean's biological pump. *Prog. Oceanogr.* **130**, 205–248. (doi:10.1016/j.pocean.2014.08.005)

2. Passow U, Carlson CA. 2012 The biological pump in a high CO2 world. *Mar. Ecol. Prog. Ser.* **470**, 249–271. (doi:10.3354/meps09985)

3. Hansell DA. 2013 Recalcitrant Dissolved Organic Carbon Fractions. *Ann. Rev. Mar. Sci.* **5**, 421–445. (doi:10.1146/annurev-marine-120710-100757)

4. Butterfield NJ. 1997 Plankton Ecology and the Proterozoic-Phanerozoic Transition. *Paleobiology* **23**, 247–262.

5. Butterfield NJ. 2009 Macroevolutionary turnover through the Ediacaran transition: Ecological and biogeochemical implications. *Geol. Soc. Spec. Publ.* **326**, 55–66. (doi:10.1144/SP326.3)

6. Lenton TM, Boyle RA, Poulton SW, Shields-Zhou GA, Butterfield NJ. 2014 Co-evolution of eukaryotes and ocean oxygenation in the Neoproterozoic era. *Nat. Geosci.* **7**, 257–265. (doi:10.1038/ngeo2108)

7. Brocks JJ, Jarrett AJM, Sirantoine E, Hallmann C, Hoshino Y, Liyanage T. 2017 The rise of algae in Cryogenian oceans and the emergence of animals. *Nature* **548**, 578–581. (doi:10.1038/nature23457)

8. Butterfield NJ. 1994 Burgess Shale-type fossils from a Lower Cambrian shallow-shelf sequence in northwestern Canada. *Nature*. **369**. (doi:10.1038/369477a0)

9. Harvey THP, Butterfield NJ. 2008 Sophisticated particle-feeding in a large Early Cambrian crustacean. *Nature* **452**, 868–871. (doi:10.1038/nature06724)

10. Antcliffe JB, Callow RHT, Brasier MD. 2014 Giving the early fossil record of sponges a squeeze. *Biol. Rev.* **89**, 972–1004. (doi:10.1111/brv.12090)

11. Botting JP, Muir LA. 2018 Early sponge evolution: A review and phylogenetic framework. *Palaeoworld*. **27**, 1–29. (doi:10.1016/j.palwor.2017.07.001)

12. Wallet E, Slater BJ, Willman S, Peel JS. 2020 Small carbonaceous fossils (SCFs) from North Greenland: new light on metazoan diversity in early Cambrian shelf environments. *Pap. Palaeontol.* , 1–31. (doi:10.1002/spp2.1347)

13. Steinberg DK, Van Mooy BAS, Buesseler KO, Boyd PW, Kobari T, Karl DM. 2008 Steinberg, Deborah K., Benjamin A. S. Van Mooy, Ken O. Buesseler, Philip W. Boyd, Toru Kobari, and

David M. Karl. Bacterial vs. zooplankton control of sinking particle flux in the ocean's twilight zone. *Limnol. Oceanogr.* **53**, 1327–1338.

14. Ortega-Hernández J. 2016 Making sense of 'lower' and 'upper' stem-group Euarthropoda, with comments on the strict use of the name Arthropoda von Siebold, 1848. *Biol. Rev.* **91**, 255–273. (doi:10.1111/brv.12168)

15. Vannier J, Chen J. 2000 The Early Cambrian colonization of pelagic niches exemplified by Isoxys (Arthropoda). *Lethaia* **33**, 295–311.

16. García-Bellido DC, Vannier J, Collins D. 2009 Soft-part preservation in two species of the arthropod *Isoxys* from the middle Cambrian Burgess Shale of British Columbia, Canada. *Acta Palaeontol. Pol.* **54**, 699–712. (doi:10.4202/app.2009.0024)

17. Legg DA, Vannier J. 2013 The affinities of the cosmopolitan arthropod *Isoxys* and its implications for the origin of arthropods. *Lethaia* **46**, 540–550. (doi:10.1111/let.12032)

18. Williams M, Siveter DJ, Peel JS. 1996 *Isoxys* (Arthropoda) from the Early Cambrian Sirius Passet Lagerstätte, North Greenland. *J. Paleontol.* **70**, 947–954. (doi:10.1017/S0022336000038646)

19. Vannier J, García-Bellido DC, Hu SX, Chen AL. 2009 Arthropod visual predators in the early pelagic ecosystem: Evidence from the Burgess Shale and Chengjiang biotas. *Proc. R. Soc. B Biol. Sci.* **276**, 2567–2574. (doi:10.1098/rspb.2009.0361)

20. Perrier V, Williams M, Siveter DJ. 2015 The fossil record and palaeoenvironmental significance of marine arthropod zooplankton. *Earth-Science Rev.* **146**, 146–162. (doi:10.1016/j.earscirev.2015.02.003)

21. Fu DJ, Zhang XL, Shu DG. 2011 Soft anatomy of the early Cambrian arthropod *Isoxys curvirostratus* from the Chengjiang biota of South China with a discussion on the origination of great appendages. *Acta Palaeontol. Pol.* **56**, 843–852. (doi:10.4202/app.2010.0090)

22. Aria C, Caron J-B. 2015 Cephalic and Limb Anatomy of a New Isoxyid from the Burgess Shale and the Role of 'Stem Bivalved Arthropods' in the Disparity of the Frontalmost Appendage. *PLoS One* **10**, e0124979. (doi:10.1371/journal.pone.0124979)

23. R Core Team. 2020 R Core Team. *R A Lang. Environ. Stat. Comput. R Found. Stat. Comput. Vienna, Austria.* See http://www.r-project.org/.

24. Vannier J, Caron J-B, Yuan J, Briggs DEG, Collins D, Zhao Y, Zhu M. 2007 *Tuzoia*: Morphology

and lifestyle of a large bivalved Arthropod of the Cambrian seas. *J. Paleontol.* **81**, 445–471.

25. Meland K, Aas PØ. 2013 A taxonomical review of the *Gnathophausia* (Crustacea, Lophogastrida), with new records from the northern mid-Atlantic ridge. *Zootaxa* **3664**, 199–225. (doi:10.11646/zootaxa.3664.2.5)

26. Bonhomme V, Picq S, Gaucherel C, Claude J. 2014 Momocs: Outline analysis using R. *J. Stat. Softw.* **56**, 1–24. (doi:10.18637/jss.v056.i13)

27. García-Bellido DC, Paterson JR, Edgecombe GD, Jago JB, Gehling JG, Lee MSY. 2009 The bivalved arthropods *Isoxys* and *Tuzoia* with soft-part preservation from the lower Cambrian Emu Bay Shale Lagerstätte (Kangaroo Island, Australia). *Palaeontology* **52**, 1221–1241. (doi:10.1111/j.1475-4983.2009.00914.x)

28. Wang Y, Huang D, Liu Q, Hu S. 2012 *Isoxys* from the Cambrian Guanshan Fauna, Yunnan Province. *Earth Sci. J. China Univ. Geosci.* **37**, 156–164.

29. Mateescu D, Abdo M. 2010 Analysis of flows past airfoils at very low Reynolds numbers. *Proc. Inst. Mech. Eng. Part G J. Aerosp. Eng.* **224**, 757–775. (doi:10.1243/09544100JAERO715)

30. Wang ZJ. 2000 Two dimensional mechanism for insect hovering. *Phys. Rev. Lett.* **85**, 2216–2219. (doi:10.1103/PhysRevLett.85.2216)

31. Cowles DL, Childress JJ, Gluckj DL. 1986 New method reveals unexpected relationship between velocity and drag in the bathypelagic mysid *Gnathophausia ingens*. *Deep. Res.* **33**, 865–880.

32. Vogel S. 1996 *Life in moving fluids: the physical biology of flow.* 2nd Editio. Princeton, New Jersey: Princeton University Press. (doi:10.2307/1352661)

33. Cowles DL, Childress JJ. 1988 Swimming Speed and Oxygen Consumption in the Bathypelagic Mysid *Gnathophausia ingens*. *Biol. Bull.* **175**, 111–121. (doi:10.2307/1541898)

34. Schoenemann B, Clarkson ENK. 2011 Eyes and vision in the Chengjiang arthropod *Isoxys* indicating adaptation to habitat. *Lethaia* **44**, 223–230. (doi:10.1111/j.1502-3931.2010.00239.x)

35. Vannier J. 2007 Early Cambrian origin of complex marine ecosystems. In *Deep-Time Perspectives on Climate Change: Marrying the Signal from Computer Models and Biological Proxies* (eds M Williams, AM Haywood, FJ Gregory, DN Schmidt), pp. 81–100. The Geological Society.

460 36. Hou X. 1987 Early Cambrian large bivalved arthropods from Chengjiang. *Acta Palaeontol. Sin.*
461 **26**, 286–297.

462 37. Fu D, Zhang X, Budd GE, Liu W, Pan X. 2014 Ontogeny and dimorphism of *Isoxys auritus*
463 (Arthropoda) from the Early Cambrian Chengjiang biota, South China. *Gondwana Res.* **25**,
464 975–982. (doi:10.1016/j.gr.2013.06.007)

465 38. Zhao FC, Zhu MY, Hu SX. 2010 Community structure and composition of the Cambrian
466 Chengjiang biota. *Sci. China Earth Sci.* **53**, 1784–1799. (doi:10.1007/s11430-010-4087-8)

467 39. Caron JB, Jackson DA. 2008 Paleoecology of the Greater Phyllopod Bed community, Burgess
468 Shale. *Palaeogeogr. Palaeoclimatol. Palaeoecol.* **258**, 222–256.
469 (doi:10.1016/j.palaeo.2007.05.023)

470 40. Allison PA. 1986 Soft-bodied animals in the fossil record: The role of decay in fragmentation
471 during transport. *Geology* **14**, 979–981.

472 41. Stein M, Peel JS, Siveter DJ, Williams M. 2010 *Isoxys* (Arthropoda) with preserved soft
473 anatomy from the Sirius Passet Lagerstätte, lower Cambrian of North Greenland. *Lethaia* **43**,
474 258–265. (doi:10.1111/j.1502-3931.2009.00189.x)

475 42. Gaines RR. 2014 Burgess Shale-type preservation and its distribution in space and time.
476 *Paleontol. Soc. Pap.* **20**, 1–24.

477 43. Lerosey-Aubril R, Kimmig J, Pates S, Skabelund J, Weug A, Ortega-Hernández J. 2020 New
478 exceptionally preserved panarthropods from the Drumian Wheeler Konservat-Lagerstätte of
479 the House Range of Utah. *Pap. Palaeontol.* **6**, 501–531. (doi:10.1002/spp2.1307)

480 44. Paterson JR, García-Bellido DC, Jago JB, Gehling JG, Lee MSY, Edgecombe GD. 2016 The Emu
481 Bay Shale Konservat-Lagerstätte: A view of Cambrian life from East Gondwana. *J. Geol. Soc.*
482 *London.* **173**, 1–11. (doi:10.1144/jgs2015-083)

483 45. Guilbaud R, Slater BJ, Poulton SW, Harvey THP, Brocks JJ, Nettersheim BJ, Butterfield NJ. 2017
484 Oxygen minimum zones in the early Cambrian ocean. *Geochemical Perspect. Lett.* **6**, 33–38.
485 (doi:10.7185/geochemlet.1806)

486 46. Harvey THP, Vélez MI, Butterfield NJ, Stanley SM. 2012 Exceptionally preserved crustaceans
487 from western Canada reveal a cryptic Cambrian radiation. *Proc. Natl. Acad. Sci. U. S. A.* **109**,
488 1589–1594. (doi:10.1073/pnas.1115244109)

489 47. Williams M, Siveter DJ, Popov LE, Vannier JMC. 2007 Biogeography and affinities of the

bradoriid arthropods: Cosmopolitan microbenthos of the Cambrian seas. *Palaeogeogr. Palaeoclimatol. Palaeoecol.* **248**, 202–232. (doi:10.1016/j.palaeo.2006.12.004)

48. Williams M, Vandenbroucke TRA, Perrier V, Siveter DJ, Servais T. 2015 A link in the chain of the Cambrian zooplankton: Bradoriid arthropods invade the water column. *Geol. Mag.* **152**, 923–934. (doi:10.1017/S0016756815000059)

49. Wolfe JM. 2017 Metamorphosis Is Ancestral for Crown Euarthropods, and Evolved in the Cambrian or Earlier. *Integr. Comp. Biol.* **57**, 499–509. (doi:10.1093/icb/icx039)

50. Selden PA, Huys R, Stephenson MH, Heward AP, Taylor PN. 2010 Crustaceans from bitumen clast in Carboniferous glacial diamictite extend fossil record of copepods. *Nat. Commun.* **1**, 1–6. (doi:10.1038/ncomms1049)

51. Hu S, Steiner M, Zhu M, Erdtmann BD, Luo H, Chen L, Weber B. 2007 Diverse pelagic predators from the Chengjiang Lagerstätte and the establishment of modern-style pelagic ecosystems in the early Cambrian. *Palaeogeogr. Palaeoclimatol. Palaeoecol.* **254**, 307–316. (doi:10.1016/j.palaeo.2007.03.044)

52. Fu D *et al.* 2019 The Qingjiang biota-A Burgess Shale-type fossil Lagerstätte from the early Cambrian of South China. *Science* . **363**, 1338–1342. (doi:10.1126/science.aau8800)

53. Rahman IA, Darroch SAF, Racicot RA, Laflamme M. 2015 Suspension feeding in the enigmatic Ediacaran organism *Tribrachidium* demonstrates complexity of Neoproterozoic ecosystems. *Sci. Adv.* **1**, e1500800. (doi:10.1126/sciadv.1500800)

54. Butterfield NJ. 2018 Oxygen, animals and aquatic bioturbation: An updated account. *Geobiology* **16**, 3–16. (doi:10.1111/gbi.12267)

55. Antcliffe JB, Jessop W, Daley AC. 2019 Prey fractionation in the Archaeocyatha and its implication for the ecology of the first animal reef systems. *Paleobiology* **45**, 652–675. (doi:10.1017/pab.2019.32)

56. Steiner M, Li G, Qian Y, Zhu M, Erdtmann BD. 2007 Neoproterozoic to Early Cambrian small shelly fossil assemblages and a revised biostratigraphic correlation of the Yangtze Platform (China). *Palaeogeogr. Palaeoclimatol. Palaeoecol.* **254**, 67–99. (doi:10.1016/j.palaeo.2007.03.046)

57. Kouchinsky A, Bengtson S, Runnegar B, Skovsted C, Steiner M, Vendrasco M. 2012 Chronology of early Cambrian biomineralization. *Geol. Mag.* **149**, 221–251. (doi:10.1017/S0016756811000720)

58. Betts MJ, Paterson JR, Jago JB, Jacquet SM, Skovsted CB, Topper TP, Brock GA. 2017 Global correlation of the early Cambrian of South Australia: Shelly fauna of the *Dailyatia odyssei* Zone. *Gondwana Res.* **46**, 240–279. (doi:10.1016/j.gr.2017.02.007)

59. Vinther J, Stein M, Longrich NR, Harper DAT. 2014 A suspension-feeding anomalocarid from the Early Cambrian. *Nature* **507**, 496–499. (doi:10.1038/nature13010)

60. Fakhraee M, Planavsky NJ, Reinhard CT. 2020 The role of environmental factors in the long-term evolution of the marine biological pump. *Nat. Geosci.* **13**, 812–816. (doi:10.1038/s41561-020-00660-6)

61. Schnetzer A, Steinberg DK. 2002 Active transport of particulate organic carbon and nitrogen by vertically migrating zooplankton in the Sargasso Sea. *Mar. Ecol. Prog. Ser.* **234**, 71–84.

62. Steinberg DK, Goldthwait SA, Hansell DA. 2002 Zooplankton vertical migration and the active transport of dissolved organic and inorganic nitrogen in the Sargasso Sea. *Deep. Res. Part I Oceanogr. Res. Pap.* **49**, 1445–1461. (doi:10.1016/S0967-0637(02)00037-7)

63. Wilson SE, Steinberg DK, Buesseler KO. 2008 Changes in fecal pellet characteristics with depth as indicators of zooplankton repackaging of particles in the mesopelagic zone of the subtropical and subarctic North Pacific Ocean. *Deep. Res. Part II Top. Stud. Oceanogr.* **55**, 1636–1647. (doi:10.1016/j.dsr2.2008.04.019)

64. Hannides CCS, Landry MR, Benitez-Nelson CR, Styles RM, Montoya JP, Karl DM. 2009 Export stoichiometry and migrant-mediated flux of phosphorus in the North Pacific Subtropical Gyre. *Deep. Res. Part I Oceanogr. Res. Pap.* **56**, 73–88. (doi:10.1016/j.dsr.2008.08.003)

65. Bollens SM, Rollwagen-Bollens G, Quenette JA, Bochdansky AB. 2011 Cascading migrations and implications for vertical fluxes in pelagic ecosystems. *J. Plankton Res.* **33**, 349–355. (doi:10.1093/plankt/fbq152)

66. Sperling EA, Frieder CA, Raman A V., Girguis PR, Levin LA, Knoll AH. 2013 Oxygen, ecology, and the Cambrian radiation of animals. *Proc. Natl. Acad. Sci. U. S. A.* **110**, 13446–13451. (doi:10.1073/pnas.1312778110)

67. Lerosey-Aubril R, Pates S. 2018 New suspension-feeding radiodont suggests evolution of microplanktivory in Cambrian macronekton. *Nat. Commun.* **9**, 1–9. (doi:10.1038/s41467-018-06229-7)

68. Servais T, Owen AW, Harper DAT, Kröger B, Munnecke A. 2010 The Great Ordovician Biodiversification Event (GOBE): The palaeoecological dimension. *Palaeogeogr.*

Palaeoclimatol. Palaeoecol. **294**, 99–119. (doi:10.1016/j.palaeo.2010.05.031)

69. Servais T *et al.* 2016 The onset of the 'Ordovician Plankton Revolution' in the late Cambrian. *Palaeogeogr. Palaeoclimatol. Palaeoecol.* **458**, 12–28. (doi:10.1016/j.palaeo.2015.11.003)

70. Van Roy P, Daley AC, Briggs DEG. 2015 Anomalocaridid trunk limb homology revealed by a giant filter-feeder with paired flaps. *Nature* **522**, 77–80. (doi:10.1038/nature14256)

71. Klug C, Kröger B, Kiessling W, Mullins G, Servais T, Frýda J, Korn D, Turner S. 2010 The Devonian nekton revolution. *Lethaia* **43**, 465–477. (doi:10.1111/j.1502-3931.2009.00206.x)

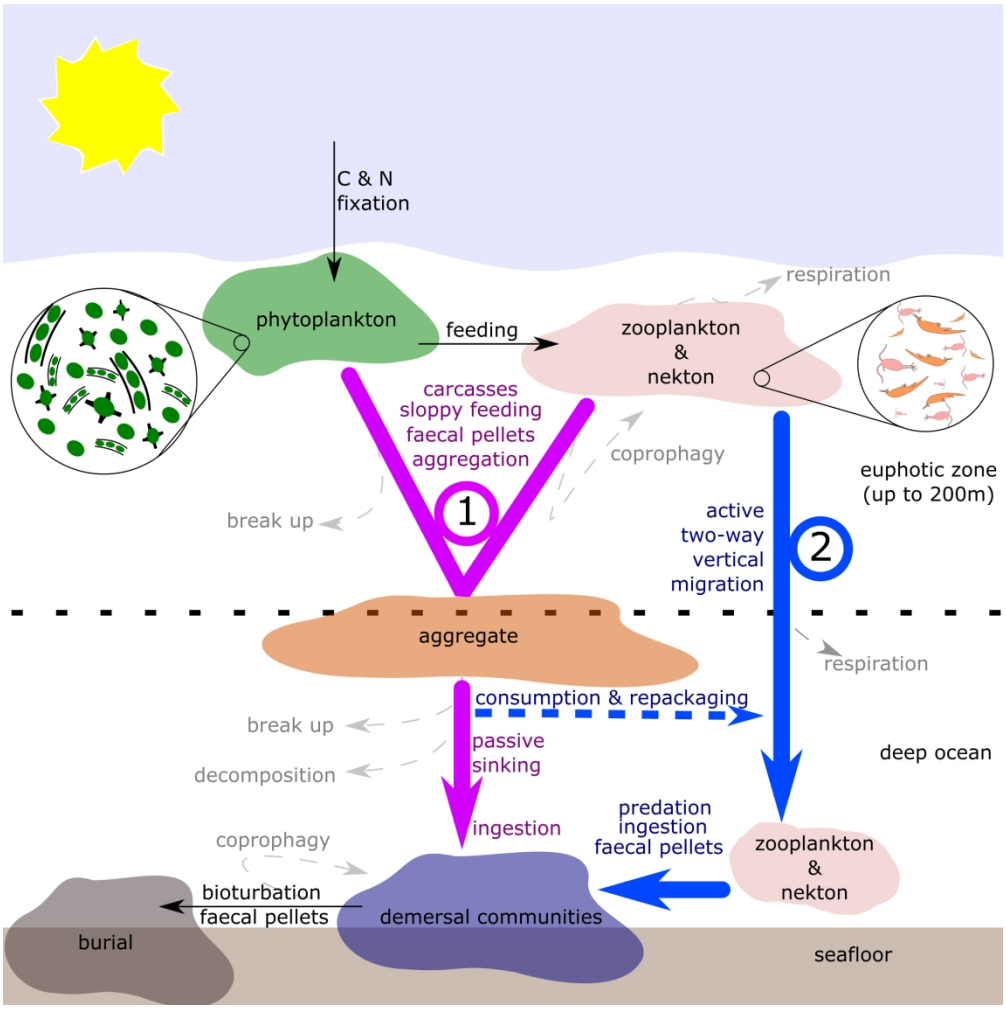

Figure 1. Simplified architecture of the modern biological pump. Arrows trace pathway of carbon (C) and nitrogen (N) and other nutrients. Numbers indicate two main biologically mediated vectors that transport nutrients fixed by phytoplankton from the surface ocean to demersal communities. 1) Aggregation vector of phytoplankton, faecal pellets, and other organic matter which sinks passively through the water column. 2) Vertical Migration vector driven by active two-way migration by metazoans.

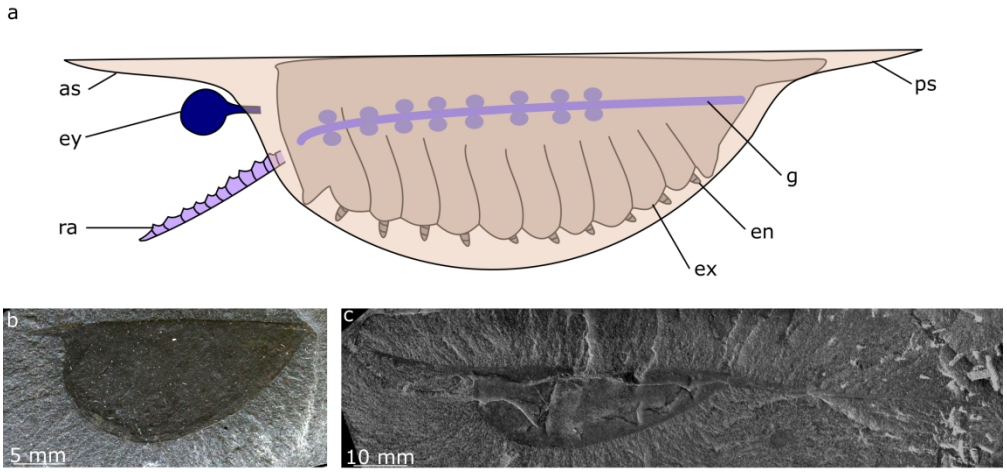

Figure 2. Morphology of Isoxys. (a) line drawing of idealised Isoxys illustrating known soft parts. (b) YPM IP 005804, Isoxys acutangulus from the Burgess Shale, British Columbia, Canada (Cambrian: Wuliuan) (credit: W. K. Sacco). (c) USNM PAL 189170, Isoxys longissimus from the Burgess Shale, British Columbia, Canada (Cambrian: Wuliuan). Image courtesy of the Smithsonian Institution (EZID: http://n2t.net/ark:/65665/m372f2a644-97c3-441c-87e2-24b1dccb2e8c, credit: Xingliang Zhang). Abbreviations: as, anterior spine; en, endopod; ex, flap like exopod; ey, eye; g, gut with paired diverticulae; ps, posterior spine; ra, raptorial appendage.

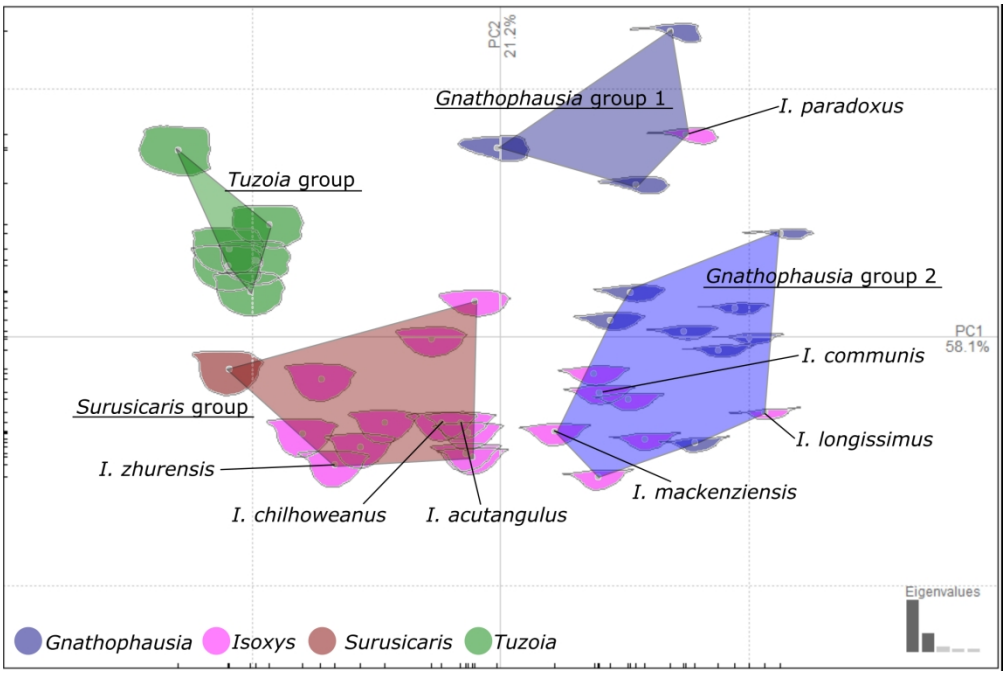

Figure 3. Principal Component Analysis of results of elliptical Fourier analysis conducted on the outlines of 11 species of Gnathophausia, 20 Isoxys, 1 Surusicaris, and 6 Tuzoia. Convex hulls indicate optimum four groupings as recovered by clustering analysis. Labelled Isoxys species chosen for subsequent hydrodynamic analysis.

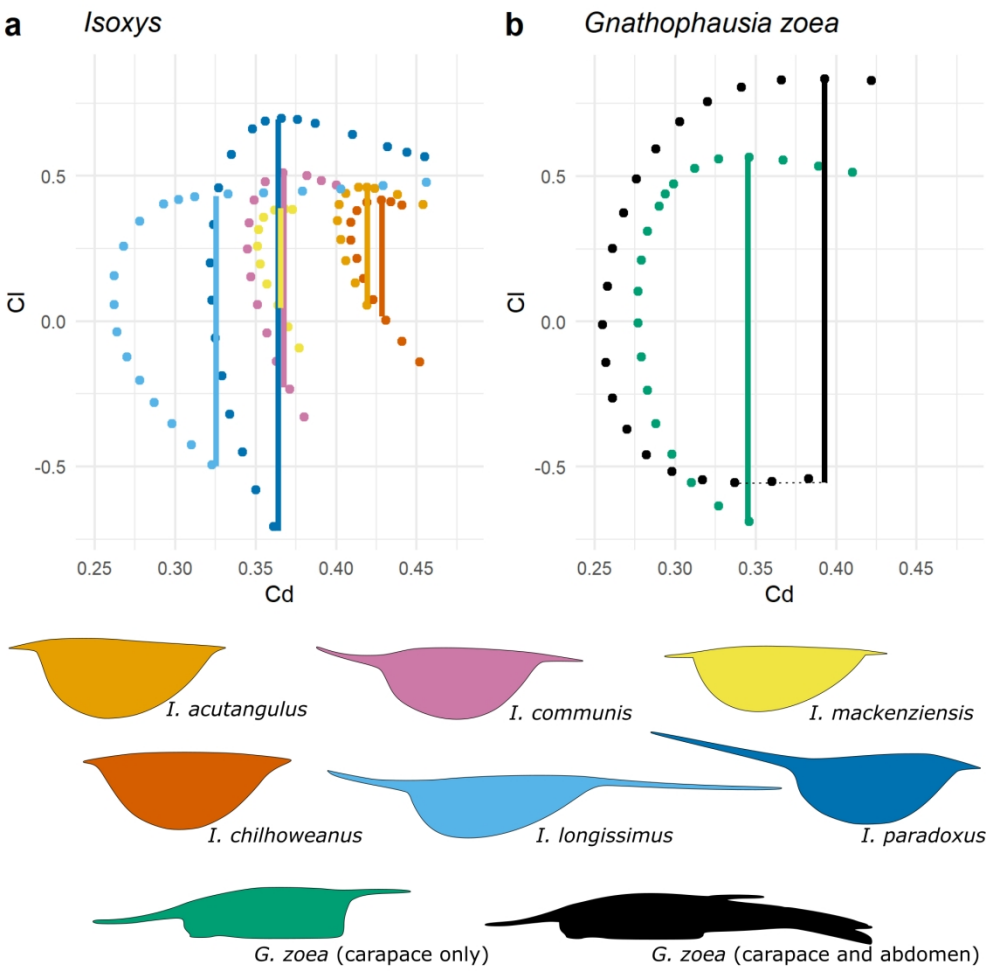

Figure 4. Drag polars (plot of Cd against Cl) of taxa analysed at Re=255 (0.75 body lengths per second for an animal 25 mm long). Each point corresponds to a single simulation at a different angle of attack. Vertical bars show range of lift coefficients. Note that flow was unsteady for Isoxys zhurensis at Re=255, and so no quantitative lift or drag coefficients were recorded. Drag polars at faster flow speeds and raw data presented in Supplemental Materials 3.

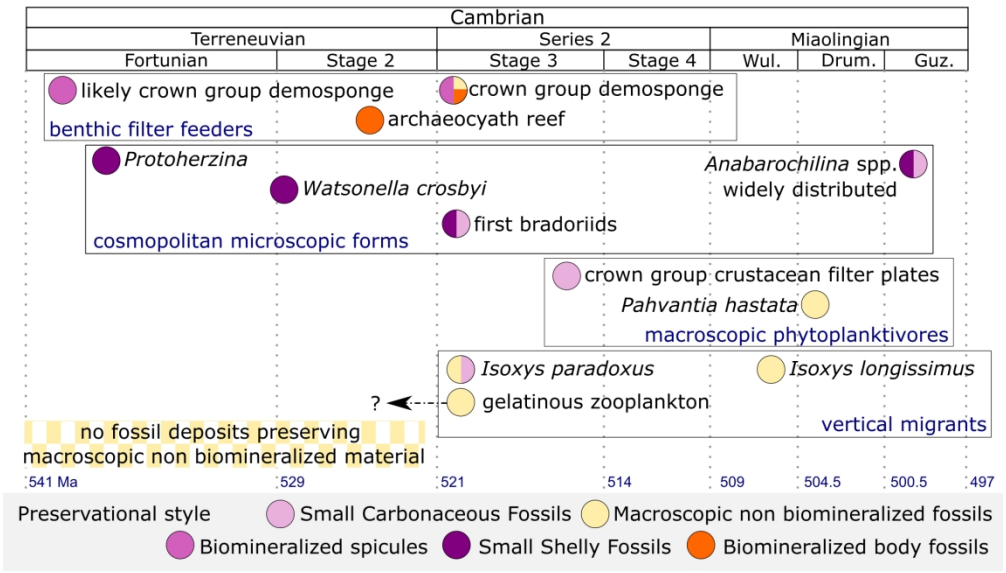

Figure 5. First known appearance in the fossil record of metazoans that impacted the biological pump. Circle colour denotes preservation style. Fossils with more than one preservation style indicated with split circles, with the preservation style that provided the oldest evidence on the left of the circle.